

UCSF

UC San Francisco Previously Published Works

Title

Functional brain basis of hypnotizability.

Permalink

<https://escholarship.org/uc/item/6nd8p7bw>

Journal

Archives of general psychiatry, 69(10)

ISSN

0003-990X

Authors

Hoeft, Fumiko
Gabrieli, John DE
Whitfield-Gabrieli, Susan
[et al.](#)

Publication Date

2012-10-01

DOI

10.1001/archgenpsychiatry.2011.2190

Peer reviewed



Published in final edited form as:

Arch Gen Psychiatry. 2012 October ; 69(10): 1064–1072. doi:10.1001/archgenpsychiatry.2011.2190.

Functional Brain Basis of Hypnotizability

Fumiko Hoeft, MD PhD^{1,2,3}, John D.E. Gabrieli, PhD⁴, Susan Whitfield-Gabrieli, BSc⁴, Brian W. Haas, PhD^{1,2}, Roland Bammer, PhD⁵, Vinod Menon, PhD¹, and David Spiegel, MD^{1,*}

¹Department of Psychiatry and Behavioral Sciences, Stanford University School of Medicine, CA 94305-5795

²Center for Interdisciplinary Brain Sciences Research (CIBSR), Stanford University School of Medicine, Stanford CA 94305-5795

³Division of Child and Adolescent Psychiatry, Department of Psychiatry, University of California San Francisco (UCSF), San Francisco, CA 94143

⁴Department of Brain and Cognitive Sciences, Massachusetts Institute of Technology, Cambridge, MA 02139

⁵Department of Radiology, Stanford University School of Medicine, Stanford CA 94305

Abstract

Context—Focused hypnotic concentration is a model for brain control over sensation and behavior. Pain and anxiety can be effectively alleviated by hypnotic suggestion, which modulates activity in brain regions associated with focused attention, but the specific neural network underlying this phenomenon is not known.

Objective—The main goal of the study was to investigate the brain basis of hypnotizability.

Design—Cross sectional, in-vivo neuroimaging study.

Setting—Academic medical center at Stanford University School of Medicine.

Patients—12 adults with high and 12 adults with low hypnotizability.

Main Outcome Measures—(1) functional MRI (fMRI) to measure functional connectivity networks at rest including default-mode, salience and executive-control networks, (2) structural T1 MRI to measure regional grey and white matter volumes, and (3) diffusion tensor imaging (DTI) to measure white matter microstructural integrity.

Results—High-compared to low-hypnotizable individuals showed greater functional connectivity between left dorsolateral prefrontal cortex (DLPFC), an executive-control region of

*CORRESPONDENCE ADDRESS: 401 Quarry Road, Office 2325, Stanford, CA, 94305-5718; dspiegel@stanford.edu; TEL: 650 723-6421 FAX: 650 498-6678.

Supplemental Material – Methods and reference list.

Contribution -- D.S., F.H., J.D.E.G., S.W.-G., V.M.: conception and design, F.H., R.B.: acquisition of data, F.H., B.W.H., S.W.-G.: analyses and interpretation of data, D.S., F.H., J.D.E.G., S.W.-G.: drafting of the manuscript, B.W.H., R.B., V.M.: critical revision of the manuscript for important intellectual content, F.H., B.W.H., S.W.-G.: statistical analysis, D.S.: obtaining funding, D.S.: administrative, technical and material support, D.S., V.M., S.W.-G., J.D.E.G., R.B.: supervision
F.H. and B.W.H. had full access to all of the data in the study and take responsibility for the integrity of the data and the accuracy of the data analysis.

the brain, and the salience network composed of the dorsal anterior cingulate cortex (dACC), anterior insula, amygdala, and ventral striatum, involved in detecting, integrating, and filtering relevant somatic, autonomic, and emotional information, using independent component analysis (ICA). Seed based analysis confirmed elevated functional coupling between the dACC and the DLPFC in high, compared to low, hypnotizables. These functional differences were not due to variation in brain structure in these regions, including regional grey and white matter volumes and white matter microstructure.

Conclusions—Our results provide novel evidence that altered functional connectivity in DLPFC and dACC may underlie hypnotizability. Future studies focusing on how these functional networks change and interact during hypnosis are warranted.

Keywords

hypnosis; hypnotizability; fMRI; resting-state functional connectivity; dorsolateral prefrontal cortex (DLPFC); dorsal anterior cingulate cortex (dACC); salience network

INTRODUCTION

Hypnosis is the oldest Western conception of psychotherapy, and a powerful means of altering pain, anxiety, and various somatic functions, even under highly stressful circumstances such as during interventional radiology procedures and breast cancer surgery.^{1–5} Hypnotic alteration of perception, most thoroughly studied in the somatosensory and visual systems, involves a top-down resetting of perceptual response itself, rather than just an alteration in post-perception processing, with reduction in early (p100) as well as late (p300) components of somatosensory event-related potential (ERP)⁶ and reduced activity of dorsal anterior cingulate (dACC) and somatosensory cortices during hypnotic analgesia.^{7–9} Hypnotic alteration of color vision results in congruent changes in blood flow in the lingual and fusiform gyri.¹⁰ Hypnotic suggestion can reduce or eliminate the well-known Stroop color-word interference phenomenon, with concomitant reduction in activation of the dACC.^{11–13} The time delay in naming a color word presented in a different color is mediated by interaction between the DLPFC and ACC.¹⁴ This is an example of how hypnosis can provide a model system for brain control over perception and behavior. Such hypnotic reduction of similar interference tasks has been shown in some studies to occur only when the hypnotic state is induced rather than as a trait difference.¹⁵

The capacity to exert this top-down processing control varies considerably among people. While most children are highly hypnotizable, substantial variation in responsiveness to hypnosis develops in adult life. Hypnotizability then becomes a stable trait, with a test-retest correlation of 0.7 over a 25 year interval.¹⁶ Despite this reliability, few meaningful correlates of this trait, either psychological or neurobiological, have been identified, despite many efforts to do so.^{11, 12, 17, 18} This remains a major challenge for the field. Clear understanding of brain functional correlates of hypnotizability would improve effective application of hypnosis in clinical settings, and provide insights into the brain basis of sensory modulation and hypnotizability.

Attention has long been described as a phenomenon of narrowing and focusing of senses by philosophers including Aristotle, Lucretius, and Descartes, which is similar to how hypnotic induction is described.¹⁹ The dACC and lateral prefrontal cortex (PFC) may contribute importantly to hypnotizability and sensory control. These regions are thought to be involved in the executive network of attention including selective attention and conflict resolution.²⁰ The dACC and lateral PFC are also targets of the mesocortical dopamine system¹¹ and hypnotizability has been found to be correlated with levels of homovanillic acid, a dopamine metabolite, in the cerebrospinal fluid.⁵⁵ High-hypnotizable individuals, but not low-hypnotizable individuals, have shown altered activation in the dACC^{7-9, 12, 21-26} and PFC^{7, 11, 22, 23} when modulating pain perception, reducing Stroop interference, and during rest when they are in versus out of hypnotic states.²⁷ This suggests that these two brain regions are involved in top-down modulation of perception during hypnosis. The implication of these findings is that there should be detectable differences in functional connectivity between these regions when comparing high to low hypnotizable individuals, and that such a difference in functional brain organization may be essential in determining who is and who is not hypnotizable and therefore who is capable of top-down sensory modulation.

To examine the functional brain basis of hypnotizability, we compared matched groups of 12 healthy high-hypnotizable (HIGH group) and 12 low-hypnotizable individuals (LOW group) on measures of (i) functional magnetic resonance imaging (fMRI) of brain blood oxygenation level dependent (BOLD) response during resting state²⁸⁻³³; (ii) high-resolution T1 structural MRI to examine voxel-based morphometry (VBM) of gray and white matter; and (iii) diffusion tensor imaging (DTI) fiber tractography to examine white matter microstructure. For the resting fMRI scan, independent component analysis (ICA) was performed and an automated, two-step process³⁴ was employed to select the component in each person that most closely matched the default-mode, salience, and executive-control resting state networks^{35, 36} (Figure 1). The *default-mode-network* involves the posterior cingulate cortex/precuneus, medial prefrontal/pregenual cingulate cortices, temporoparietal regions, and medial temporal lobes, and is implicated in episodic memory retrieval, self-reflection, mental imagery, and stream-of-consciousness processing.^{32, 37-39} The *salience network* includes the dACC, frontoinsula cortices, and limbic structures, and is involved in detecting, integrating, and filtering relevant somatic (interoceptive), autonomic, and emotional information.^{35, 39} The *executive-control network* involves the dorsolateral prefrontal cortex (DLPFC) and lateral parietal cortices and is required for the selection and maintenance in working memory of relevant information necessary for action preparation.^{35, 39} We hypothesized that there would be functional differences in and between brain networks that involve regions associated with attention and executive-control (ACC, DLPFC) between the HIGH and LOW groups.

METHODS (see also Supplementary Methods)

Subjects

Twenty-four subjects (12 high-hypnotizable (HIGH) and 12 low-hypnotizable (LOW) individuals) participated as paid volunteers recruited through lectures about hypnosis and advertisements asking “Are you interested in finding out how hypnotizable you are?” (Table

1). The subjects were included in the HIGH group if they scored 7–10 and in the Low group if they scored 0–3 on the Hypnotic Induction Profile (HIP; range 0 to 10).⁴⁰ This is a structured hypnotic induction assessing subjective and behavioral response to hypnotic suggestion of: 1) dissociation, 2) levitation of the hand following its being lowered; 3) a sense of involuntariness during the elevation of the hand; 4) response to the signal cutting off the instruction of lightness and movement; and 5) a sensory alteration of floating, lightness, or buoyancy. Handedness was determined using the Edinburgh Handedness Questionnaire – Revised.⁴¹ Subjects had no neurological or psychiatric disorders, were not on any medication, and had no contraindications to MRI. By design, there was a significant difference in HIP scores between the two groups ($t_{(22)} = 20.24$, $p < 0.001$). There were no significant differences in age, handedness, or gender between the groups (gender and handedness: $\chi^2_{(1)} = 0$, $p = 1.00$; age: $t_{(22)} = 1.61$, $p = 0.12$) (Table 1). The median duration between these assessments and the MRI session were 2 months and 1 days (range 0 months to 8 months and 20 days). The study was approved by the Stanford University Panel on Human Subjects in Medical Research, and informed consent was obtained.

Functional Magnetic Resonance Imaging (fMRI)

Image Acquisition—All functional and structural MRIs of each subject’s brain were acquired at the Lucas Center (Stanford University, Palo Alto, CA USA) using a 1.5T GE Signa scanner and a standard GE whole head coil (Lx platform; GE Medical Systems, Milwaukee, WI USA). Subjects underwent a 6-min resting-state scan in which they were given no specific instructions except to keep their eyes closed and hold still: T2* weighted gradient echo spiral pulse sequence⁴², 30 axial slices (AC-PC aligned), 4mm thick, 1mm skip, repetition time (TR) 2500msec, time to echo (TE) 40msec, flip angle 85°, 1 interleave, field of view (FOV) 22cm, and matrix size 64x64.

Data Processing: Data were pre-processed using Statistical Parametric Mapping (SPM2; <http://www.fil.ion.ucl.ac.uk/spm>) using standard methods. Specifically, images were slice-time corrected, realigned and normalized to the functional (echo planar image) Montreal Neurological Institute (MNI) template (12-parameter affine transformation, nonlinear normalization using 7×8×7 basis functions, resampled to 2mm voxel)⁴³. Images were then smoothed with an isotropic Gaussian kernel of 4 mm full-width at half-maximum (FWHM). Independent Component Analysis (ICA) was then performed on these images using FSL melodic software (www.fmrib.ox.ac.uk/fsl/melodic2/index.html).

Component Selection⁴⁴: An automated, two-step process as described in ³⁴ was then employed to select the component in each subject that most closely matched the salience, default-mode, and executive-control networks using Matlab (Mathworks, Natick, MA) (Figure 1). First, if high-frequency signal (< 0.1 Hz) constituted 50 % or more of the total power in the Fourier spectrum, a frequency filter was applied to remove any components. Next, templates of these networks derived from a separate group of 14 healthy controls (Figure 1B in ³⁴) were used to select the “best-fit” of the remaining low-frequency components in each subject. This was done by using a nonlinear template-matching procedure that involves taking the average z-score of voxels falling within the template

minus the average z -score of voxels outside the template and selecting the component in which this difference (the goodness-of-fit) was the greatest.

Goodness-Of-Fit Scores⁴⁴: In order to test how well this approach works in selecting uniquely representative components and to be certain that the approach did not differ across groups, we compared the mean goodness-of-fit scores for the best-fit component and the second best-fit component within and across groups using paired and two-sample t -tests respectively. All group analyses were performed on the subjects' "best-fit" component images. Across the 24 subjects the mean goodness-of-fit score was 0.99 (standard deviation, SD 0.36) for the salience network best-fit component, which was significantly larger than the second best-fit component (0.65, SD 0.21; $t_{(23)} = 5.55$, $p < 0.001$). The two groups did not differ in their mean goodness-of-fit score for the best-fit component (HIGH 1.06, SD 0.40; LOW 0.97, SD 0.35; $t_{(22)} = 0.62$, $p = 0.54$) or the second best-fit component (HIGH 0.70, SD 0.19; LOW 0.62, SD 0.25; $t_{(22)} = 0.82$, $p = 0.42$). These data suggest that our automated selection procedure was effective in selecting a unique component in each subject that corresponds to the salience network and further that the selection procedure worked equally well across the two groups. The default-mode and executive-control networks showed similar effects (**default-mode-network**: HIGH: mean = 1.96, SD = 0.69 LOW: mean = 1.83, SD = 0.56, $t_{(22)} = 0.50$, $p = 0.62$, between 1st and 2nd best-fit components: $t_{(23)} = 6.9$, $p < 0.001$; **executive-control network**: HIGH: mean = 1.58, SD = 0.65, LOW: mean = 1.65, SD = 0.69, $t_{(22)} = 0.24$, $p = 0.81$, between 1st and 2nd best-fit components: $t_{(23)} = 6.7$, $p < 0.001$).

Statistical Analysis: First, using SPM, decomposed spatial maps from the selected components were submitted to one-sample and two-sample t -tests to compare the salience, default-mode, and executive-control networks between the two groups. Significant clusters were determined using the joint expected probability distribution⁴⁵ with height ($p < 0.01$) and cluster extent ($p < 0.01$ family-wise error [FWE] corrected) thresholds. To obtain a measure of effect size of the salience network, we created a whole-brain Cohen's d map comparing the HIGH and LOW groups.⁴⁶ Statistical maps were superimposed on T1 templates using MRICro and cluster locations interpreted using known neuroanatomical landmarks. Statistical images were overlaid onto the MRICro (<http://www.sph.sc.edu/comd/rorden/micro.html>) template image for viewing. To aid in localization, peak coordinates of brain regions with significant effects were converted from MNI to Talairach space using the mni2tal function (<http://www.mrc-cbu.cam.ac.uk/Imaging/Common/mnispace.shtml>). Brain regions were identified from these X, Y, Z coordinates using Talairach Daemon (Research Imaging Center, University of Texas Health Science Center in San Antonio (RIC UTHSCSA, TX USA) and confirmed with the Talairach atlas⁴⁷.

Further, confirmatory seed-based functional connectivity analyses were performed by calculating Pearson's correlation coefficients using extracted time-series of the DLPFC and dACC regions defined from the ICA between-group analyses of the SN. This was calculated for each subject separately, and by removing spurious sources of variance similar to⁴⁸ by using white matter and cerebro-spinal fluid (CSF) time-series. Fisher r -to- z transformation was performed to compare difference between the HIGH and LOW groups.

Finally, decomposed time-series from selected components for the DMN, SN and ECN were correlated with one another to examine the relationships between different networks in Matlab. This was calculated for each subject separately. Fisher r-to-z transformation was performed and compared between the HIGH and LOW groups.

Voxel-Based Morphometry (VBM)

Image Acquisition—A three-dimensional, high-resolution T1-weighted anatomic gradient and a receptive field-SPGR, MRI sequence with the following parameters was used: TR=9ms, TE=1.8ms, flip angle=15°; number of excitations=1; matrix size=220x220; FOV=22cm; 124 contiguous slices of 1.2mm-width.

Data Processing: Data processing and statistical analysis was performed using SPM2. Optimized and modulated VBM techniques were performed as described in Good et al.⁴⁹

Statistical Analyses: Between-group differences of regional gray and white matters were compared using independent sample t-tests. Significant clusters of activation were determined using the joint expected probability distribution⁴⁵ with height ($p < 0.01$) and extent ($p < 0.01$) thresholds, FWE corrected at the whole-brain level and for non-isotropic smoothness. A lenient threshold of $p = 0.001$ uncorrected was also used to confirm when no significant effects were found at the corrected threshold.

Diffusion-Tensor Imaging (DTI)

DTI Image Acquisition—The DTI sequence was based on a single-shot spin-echo echo-planar imaging sequence with diffusion sensitizing gradients applied on either side of the 180° refocusing pulse.⁵⁰ Imaging parameters for the diffusion-weighted sequence were as follows: FOV=26cm, matrix size=128x128, TE=58.1ms, TR=4500ms; 60 axial-oblique slices; slice thickness=2mm. Diffusion weighting was $b = 815 \text{ s/mm}^2$. In addition, two reference measurements (b_0 scans) were performed and averaged for each slice after removing the diffusion sensitizing gradients. Diffusion was measured along twelve non-collinear directions. This pattern was repeated six times for each slice, with the sign of all diffusion gradients inverted for odd repetitions.

DTI Image Processing: First diffusion weighted images were corrected for eddy current distortions and head motion using linear image registration (Automated Image Registration (AIR) algorithm).⁵¹ Thereafter, DtiStudio⁵² (<https://www.dtistudio.org/>) was used.

Diffusion-Tensor Fiber-Tracking: All analyses were performed using DtiStudio⁵³ by a researcher blind to the subject's group assignment. Fiber-tracking was performed using Fiber Assignment by Continuous Tracking (FACT) method,⁵⁴ and regions of interest (ROIs, i.e., the left DLPFC and dACC) were derived based on regions that were significant during the resting state functional connectivity results ($p < 0.05$ corrected).

Descriptive statistics including fractional anisotropy (FA), apparent diffusion coefficient (ADC), fiber volume (in voxels) and density (number of fibers per voxel) for each selected group of fibers were collected and included in the overall between-group statistical analysis.

Planned between-group comparisons (HIGH vs. LOW) were conducted using two-sample t-tests with a statistical threshold of $p < 0.05$ (two-tailed).

RESULTS

First, using ICA, direct comparison of salience network ICA maps between the HIGH hypnotizable, relative to the LOW group, showed increased functional connectivity between one brain region that is central to the salience network, the dACC, and the left DLPFC ($p < 0.01$ corrected; Figure 2A left panel, Table 2). Whole-brain Cohen's *d* map comparing the HIGH and LOW groups for the salience network showed large effect sizes in these left DLPFC and the dACC (bilateral with peak centered on left hemisphere) regions ($d's > 0.8$; Figure 2A right panel). In no brain region did the HIGH group display reduced connectivity in the salience network compared to the LOW group.

These results were supplemented by the HIGH group showing left DLPFC, normally found as part of the executive control network, incorporated into the salience network during rest which included the ACC, whereas this did not occur in the LOW group ($p < 0.01$ corrected; Figure 2B). The two groups did not differ reliably in functional connectivity within the default-mode or executive-control networks.

Confirmatory seed-based analyses were performed by examining temporal associations between time-series of left DLPFC and dACC regions. There was significantly greater functional connectivity between left DLPFC and dACC in the HIGH compared to the LOW group (HIGH: mean $Z = 0.60$, LOW: mean $Z = 0.23$, $p < 0.001$, Figure 2C).

Further, Independent Components Analysis (ICA) time-series extracted for each participant from the executive control and salience networks showed a consistent profile of higher correlation in the HIGH compared to the LOW group (HIGH: mean $Z = 0.75$, LOW: mean $Z = 0.10$, between-group comparison: $p = 0.066$). There was no significant difference in functional connectivity between the default-mode and both the salience ($p = 0.21$) and the executive-control networks ($p = 0.17$).

The HIGH and LOW groups did not differ on any measures of brain structure, including total volumes (gray: $t^{(22)} = 0.17$, $p = 0.87$; white: $t^{(22)} = 0.47$, $p = 0.64$) or regional voxel-by-voxel volumes using VBM ($p's > 0.01$ corrected). Differences were found in the parietal, temporal and cerebellar regions only when the threshold was reduced to $p = 0.001$ uncorrected, but even then not in the dACC or DLPFC, where there were differences in functional connectivity between the HIGH and LOW groups. DTI analyses of FA (typically representing greater white matter integrity), ADC (typically representing white matter organization), fiber volume (in voxels) and density (number of fibers per voxel) within the fiber-tracts identified by placing seeds in either the DLPFC, dACC or both, identified from the functional connectivity analysis, showed no significant differences between groups (all $p's > 0.1$). This suggests that the observed differences in *functional* connectivity were not due to gross regional volumetric or *structural* connectivity differences.

DISCUSSION

We found resting state functional brain differences related to hypnotizability. High-versus low-hypnotizable individuals showed significantly greater involvement the DLPFC region, a key node of the executive-control network, in the salience network. Convergent on these findings from ICA, seed based analysis confirmed elevated coupling between the dACC and the DLPFC in high, compared to low, hypnotizables. These findings provide novel evidence for cross-network coupling in high hypnotizable individuals. Additional analyses revealed that functional differences were not associated with structural (regional gray and white matter VBM and white matter DTI) differences.

Activation of dACC and DLPFC has been observed during hypnotic task performance. Hypnotically imagined pain is accompanied by activation in thalamus, dACC and DLPFC as well as insula and parietal cortex.²³ Hypnotically imagined handgrip activation also results in increased activity in dACC and insula among high hypnotizables.⁵⁵ Hypnotic inhibition of Stroop interference is associated with reduced dACC activation,¹² as is hypnotic analgesia directed at the affective component of pain.⁵⁶ Hypnotic analgesia is associated with reduced activity of the dACC⁵⁷ and hypnotically-related increases in functional connectivity between primary somatosensory area (S1) and anterior insular and prefrontal cortices. Further, high-, but not low-hypnotizable, individuals show differences during rest in hypnotic versus non-hypnotic states, and these differences are reduced activation in dACC and PFC, including left DLPFC²⁷

While the subjects in this study were not asked to engage in hypnotic tasks, the greater resting state coordination of brain areas associated with conflict detection / focusing of attention (dACC) and motor planning, integration of sensory information, regulation of intellectual function, and working memory (DLPFC) observed among high hypnotizables involve two key components of the anterior attentional system.^{13, 58} Co-activation of the salience and executive control networks, of which the DLPFC is a key node are consistent with evidence that the natural tendency to become intensely absorbed in experience outside of hypnosis is correlated with hypnotizability,⁵⁹⁻⁶¹ leading to the description of hypnosis as “effortless experiencing.”⁶² The next step in this research would involve fMRI assessment during hypnotic states. Based on the current findings, the prediction would be that the combination of focused attention and conflict reduction that makes hypnosis an effective form of top-down control over sensation and motor function would involve networks such as the executive control and salience networks during hypnosis among high hypnotizables, but not following hypnotic induction among lows. Further, working memory influence on conflict detection allows for hypnotic modulation of perception using instructed imagery, for example in the visual⁶³ and somatosensory^{9, 64, 65} systems.

Genetic and neurotransmitter findings are also consistent with the possibility that the DLPFC and dACC play an important role in hypnotizability. These regions are rich in dopamine-mediated synapses. Hypnotizability is correlated with levels of homovanillic acid, a dopamine metabolite, in the cerebrospinal fluid.⁶⁶ Catechol-*O*-methyl transferase (COMT), a gene that affects dopamine function, influences prefrontal executive cognition,⁶⁷ and an association between a COMT polymorphism and hypnotizability has been

shown.^{11, 18, 68 69} The val/met heterozygous form is associated with higher hypnotizability, except in one study in which those with the val/val polymorphism were even higher,⁶⁹ and may allow for greater frontal lobe dopamine-mediated flexibility in figure/ground attention, representing enhanced attentional control and therefore greater task engagement.

These findings provide new evidence that hypnosis and the related ability to modulate sensory experience, including pain and anxiety, involves focused attention and concentration, and that those capable of it have more coordination between areas that integrate attention, emotion, action, and intention. Paradoxically, hypnosis is often seen as submission or a loss of control, despite the fact that high-hypnotizable individuals show surprisingly enhanced control over sensory, motor, and somatic function. Yet they do this with a sense of involuntariness, somehow dissociated from their own abilities, as though they were observing rather than deliberately enacting them. It would seem that the enhanced cognitive control is associated with reduced conflict detection – absorption in the task coupled with dissociation of other competing tasks, as well as reduced awareness of agency in accomplishing them, which has been referred to as “self-altering attention.”¹⁷ The data from this study would support a description of hypnosis as “conflict-free attention and intention.”

Increased functional connectivity between dACC and DLPFC indicates more coordinated activity between these brain regions in high-hypnotizable people. The hypnotic experience may involve enhanced focus of attention through linking working memory more closely with attention, thereby reducing the load on conflict detection. This could account for controlled dissociative experience in hypnosis, in which perceptions ordinarily available to consciousness are put outside of conscious awareness (e.g. analgesia^{4, 9, 56} or alteration of color perception¹⁰), despite the apparent incongruity of this sensory alteration. Furthermore, the intensity of engagement during hypnosis reduces self-consciousness about the experience, which further reinforces the intensity of the experience itself at the expense of awareness of the context in which the experience occurs.⁷⁰ Thus reduced conflict detection may in turn facilitate the focusing and intensity of attentional modulation of perception. The results are of particular interest in that they highlight the role of two brain regions that have been associated with executive-control (DLPFC) and salience (dACC) in individuals with high hypnotizability.^{35, 36} Studies are variable in whether the DLPFC appears to be part of the salience network,³⁹ and this variability may reflect such individual differences among participants in any given study.

There are several important limitations to these findings that should be addressed in future studies. While some have criticized the HIP as a tool for screening individuals with high and low hypnotizability, interrater reliability ranges between .68–76,^{71–73} and scores on the HIP are moderately and significantly correlated with scores on the Stanford Hypnotic Susceptibility Scale (SHSS) at the same level that any one item on the SHSS is with the overall score.^{74 75 76} Further, HIP scores are significantly higher among those with post-traumatic stress disorder^{77 78 79}, and pseudoepilepsy⁸⁰, significantly lower among those with schizophrenia^{73 81 82}, are positively associated with the trait of absorption⁵⁹, and they predict outcome of hypnotic treatment for smoking control⁸³ and flying phobia.⁸⁴ Second, we examined resting state differences without behavioral measures, so we have no evidence

regarding the effect of hypnotic induction or specific tasks. However, the fact that we observed robust resting state differences despite the absence of tasks designed to elicit activation in specific brain regions suggests fundamental functional brain differences even in the absence of a task between the two groups. Third, despite the absence of any hypnotic instruction during the scanning (subjects were simply asked to close their eyes and lie still), because hypnotizability assessment was conducted prior to scanning (though it was on average 2 months earlier), some subjects may have inferred that a hypnotic-like state was being studied during the imaging. Fourth, the sample was of modest size. Fifth, although we focused on ICA-based networks with complementary seed-based analysis of functional coupling between the dACC and DLPFC, other approaches such as graph theoretical analysis may provide additional insights into brain systems underlying hypnotizability. Finally, while we used the terms executive control and salience networks in defining the networks based on prior work^{35, 36}, depending on the analysis method and study, the key regions in our study such as the dACC may also be considered part of an attentional network. Further, the effect of increased left DLPFC – dACC connectivity in highly hypnotizable individuals may extend beyond hypnotizability to other domains of attention and may be non-specific. We did not explore this in our study. Other analytical approaches and inclusion of behavioral measures may help identify the networks that differ dependent on the trait of hypnotizability.

These results provide a neural basis for an important trait difference, which is an area of growing importance in neuropsychology.^{85, 86, 87} While enhanced psychological and somatic control has been observed with the use of mindfulness meditation, along with increases in left frontal activation,^{88, 89} our findings differ in emphasizing co-activation of DLPFC and dACC, which suggests that future research might examine such a potential difference between the two techniques. Mindfulness is considered a practice that must be developed with considerable time and effort. Here we observe differences in hypnotizability that are unrelated to training or experience in hypnosis, suggesting a difference in cognitive style that is available to some more than others, independent of training.

These results are compatible with the idea that high-hypnotizable individuals have an exceptional capacity for top-down sensory control via coordinated activity of the DLPFC and dACC, which is illustrated by reductions in the affective components of pain via reduced dACC activity during one type of analgesia and in Stroop interference, and in alteration of sensory cortex response to stimuli during hypnotic analgesia that reduces the sensory component of pain, or modulates color processing. Hypnotizability involves a combination of cognitive control and engagement – self-altering attention – that may be mediated by enhanced frontal – anterior cingulate functional connectivity. The co-activation of these regions could provide the brain basis for helping patients to enhance pain and anxiety control and for clinically relevant symptom control including the effects of social support, emotional control, and placebo effects.

Supplementary Material

Refer to Web version on PubMed Central for supplementary material.

ACKNOWLEDGMENT

This study was supported by grants from the Nissan Research Center (D.S.), the Randolph H. Chase, M. D. Fund II (D.S.), the Jay and Rose Phillips Family Foundation (D.S.) and P41 RR09784 (P.I. Dr. Gary Glover). The funding agencies played no role in the acquisition of data, analyses and interpretation of results. Authors declare no conflict of interest. We thank Dr. Lisa Butler, Liz Seibert, and Emily Dennis for their invaluable work on the project.

REFERENCES

1. Lang EV, Berbaum KS, Faintuch S, Hatsiopolou O, Halsey N, Li X, Berbaum ML, Laser E, Baum J. Adjunctive self-hypnotic relaxation for outpatient medical procedures: a prospective randomized trial with women undergoing large core breast biopsy. *Pain*. 2006; 126(1–3):155–164. [PubMed: 16959427]
2. Lang EV, Benotsch EG, Fick LJ, Lutgendorf S, Berbaum ML, Berbaum KS, Logan H, Spiegel D. Adjunctive non-pharmacological analgesia for invasive medical procedures: a randomised trial. *Lancet*. 2000; 355(9214):1486–1490. [PubMed: 10801169]
3. Montgomery GH, Bovbjerg DH, Schnur JB, David D, Goldfarb A, Weltz CR, Schechter C, Graff-Zivin J, Tatrow K, Price DD, Silverstein JH. A randomized clinical trial of a brief hypnosis intervention to control side effects in breast surgery patients. *J Natl Cancer Inst*. 2007; 99(17):1304–1312. [PubMed: 17728216]
4. Lee JS, Spiegel D, Kim SB, Lee JH, Kim SI, Yang BH, Choi JH, Kho YC, Nam JH. Fractal analysis of EEG in hypnosis and its relationship with hypnotizability. *Int J Clin Exp Hypn*. 2007; 55(1):14–31. [PubMed: 17135061]
5. Colgan SM, Faragher EB, Whorwell PJ. Controlled trial of hypnotherapy in relapse prevention of duodenal ulceration. *Lancet*. 1988; 1(8598):1299–1300. [PubMed: 2897556]
6. Spiegel D, Bierre P, Rootenberg J. Hypnotic alteration of somatosensory perception. 711. *Am J Psychiatry*. 1989; 146(6):749–754. [PubMed: 2729425]
7. Rainville P, Hofbauer RK, Paus T, Duncan GH, Bushnell MC, Price DD. Cerebral.
8. Faymonville ME, Laureys S, Degueldre C, DelFio G, Luxen A, Franck G, Lamy M, Maquet P. Neural mechanisms of antinociceptive effects of hypnosis. *Anesthesiology*. 2000; 92(5):1257–1267. [PubMed: 10781270]
9. Rainville P, Hofbauer RK, Bushnell MC, Duncan GH, Price DD. Hypnosis modulates activity in brain structures involved in the regulation of consciousness. *J Cogn Neurosci*. 2002; 14(6):887–901. [PubMed: 12191456]
10. Kosslyn SM, Thompson WL, Costantini-Ferrando MF, Alpert NM, Spiegel D. Hypnotic visual illusion alters color processing in the brain. *Am J Psychiatry*. 2000; 157(8):1279–1284. [PubMed: 10910791]
11. Raz A. Attention and hypnosis: neural substrates and genetic associations of two converging processes. *Int J Clin Exp Hypn*. 2005; 53(3):237–258. [PubMed: 16076662]
12. Raz A, Fan J, Posner MI. Hypnotic suggestion reduces conflict in the human brain. *Proc Natl Acad Sci U S A*. 2005; 102(28):9978–9983. [PubMed: 15994228]
13. Raz A, Shapiro T, Fan J, Posner MI. Hypnotic suggestion and the modulation of Stroop interference. *Arch Gen Psychiatry*. 2002; 59(12):1155–1161. [PubMed: 12470132]
14. Morishima Y, Okuda J, Sakai K. Reactive mechanism of cognitive control system. *Cereb Cortex*. 2010; 20(11):2675–2683. [PubMed: 20154012]
15. Iani C, Ricci F, Baroni G, Rubichi S. Attention control and susceptibility to hypnosis. *Conscious Cogn*. 2009; 18(4):856–863. [PubMed: 19648030]
16. Piccione C, Hilgard ER, Zimbardo PG. On the degree of stability of measured hypnotizability over a 25-year period. *J Pers Soc Psychol*. 1989; 56(2):289–295. [PubMed: 2926631]
17. Tellegen A, Atkinson G. Openness to absorbing and self-altering experiences (“absorption”), a trait related to hypnotic susceptibility. *J Abnorm Psychol*. 1974; 83(3):268–277. [PubMed: 4844914]
18. Lichtenberg P, Bachner-Melman R, Ebstein RP, Crawford HJ. Hypnotic susceptibility: multidimensional relationships with Cloninger's Tridimensional Personality Questionnaire, COMT

- polymorphisms, absorption, and attentional characteristics. *Int J Clin Exp Hypn*. 2004; 52(1):47–72. [PubMed: 14768969]
19. Karlin RA. Hypnotizability and attention. *J Abnorm Psychol*. 1979; 88(1):92–95. [PubMed: 422807]
 20. Pochon JB, Riis J, Sanfey AG, Nystrom LE, Cohen JD. Functional imaging of decision conflict. *J Neurosci*. 2008; 28(13):3468–3473. [PubMed: 18367612]
 21. Spiegel D, King R. Hypnotizability and CSF HVA levels among psychiatric patients. *Biol Psychiatry*. 1992; 31(1):95–98. [PubMed: 1543801]
 22. Oldfield RC. The assessment and analysis of handedness: the Edinburgh inventory. *Neuropsychologia*. 1971; 9(1):97–113. [PubMed: 5146491]
 23. Szechtman H, Woody E, Bowers KS, Nahmias C. Where the imaginal appears real: a positron emission tomography study of auditory hallucinations. *Proc Natl Acad Sci USA*. 1998; 95(4):1956–1960. [PubMed: 9465124]
 24. Maquet P, Faymonville ME, Degueldre C, Delfiore G, Franck G, Luxen A, Lamy M. Functional neuroanatomy of hypnotic state. *Biol Psychiatry*. 1999; 45(3):327–333. [PubMed: 10023510]
 25. Derbyshire SW, Whalley MG, Stenger VA, Oakley DA. Cerebral activation during hypnotically induced and imagined pain. *Neuroimage*. 2004; 23(1):392–401. [PubMed: 15325387]
 26. Schulz-Stübner S, Krings T, Meister IG, Rex S, Thron A, Rossaint R. Clinical hypnosis modulates functional magnetic resonance imaging signal intensities and pain perception in a thermal stimulation paradigm. *Reg Anesth Pain Med*. 2004; 29(6):549–556. [PubMed: 15635514]
 27. Egner T, Jamieson G, Gruzeliier J. Hypnosis decouples cognitive control from conflict monitoring processes of the frontal lobe. *Neuroimage*. 2005; 27(4):969–978. [PubMed: 15964211]
 28. Raji TT, Numminen J, Narvanen S, Hiltunen J, Hari R. Brain correlates of subjective reality of physically and psychologically induced pain. *Proc Natl Acad Sci USA*. 2005; 102(6):2147–2151. [PubMed: 15684052]
 29. McGeown WJ, Mazzoni G, Venneri A, Kirsch I. Hypnotic induction decreases anterior default mode activity. *Conscious Cogn*. 2009; 18(4):848–855. [PubMed: 19782614]
 30. Biswal BB, Mennes M, Zuo XN, Gohel S, Kelly C, Smith SM, Beckmann CF, Adelstein JS, Buckner RL, Colcombe S, Dogonowski AM, Ernst M, Fair D, Hampson M, Hoptman MJ, Hyde JS, Kiviniemi VJ, Kotter R, Li SJ, Lin CP, Lowe MJ, Mac-kay C, Madden DJ, Madsen KH, Margulies DS, Mayberg HS, McMahon K, Monk CS, Mostofsky SH, Nagel BJ, Pekar JJ, Peltier SJ, Petersen SE, Riedl V, Rom-bouts SA, Rypma B, Schlaggar BL, Schmidt S, Seidler RD, Siegle GJ, Sorg C, Teng GJ, Veijola J, Villringer A, Walter M, Wang L, Weng XC, Whitfield-Gabrieli S, Williamson P, Windischberger C, Zang YF, Zhang HY, Castellanos FX, Mil-ham MP. Toward discovery science of human brain function. *Proc Natl Acad Sci USA*. 2010; 107(10):4734–4739. [PubMed: 20176931]
 31. Van Dijk KR, Hedden T, Venkataraman A, Evans KC, Lazar SW, Buckner RL. Intrinsic functional connectivity as a tool for human connectomics: theory, properties, and optimization. *J Neurophysiol*. 2010; 103(1):297–321. [PubMed: 19889849]
 32. Fox MD, Raichle ME. Spontaneous fluctuations in brain activity observed with functional magnetic resonance imaging. *Nat Rev Neurosci*. 2007; 8(9):700. [PubMed: 17704812]
 33. Raichle ME, MacLeod AM, Snyder AZ, Powers WJ, Gusnard DA, Shulman GL. A default mode of brain function. *Proc Natl Acad Sci USA*. 2001; 98(2):676- mechanisms of hypnotic induction and suggestion. *J Cogn Neurosci*. 1999; 11(1):110–125. 682. [PubMed: 9950718]
 34. Raichle ME. The brain's dark energy. *Sci Am*. 2010; 302(3):44–49. [PubMed: 20184182]
 35. Greicius MD, Srivastava G, Reiss AL, Menon V. Default-mode network activity distinguishes Alzheimer's disease from healthy aging: evidence from functional MRI. *Proc Natl Acad Sci USA*. 2004; 101(13):4637–4642. [PubMed: 15070770]
 36. Seeley WW, Menon V, Schatzberg AF, Keller J, Glover GH, Kenna H, Reiss AL, Greicius MD. Dissociable intrinsic connectivity networks for salience processing and executive control. *J Neurosci*. 2007; 27(9):2349–2356. [PubMed: 17329432]
 37. Sridharan D, Levitin DJ, Menon V. A critical role for the right fronto-insular cortex in switching between central-executive and default-mode networks. *Proc Natl Acad Sci USA*. 2008; 105(34):12569–12574. [PubMed: 18723676]

38. Greicius MD, Krasnow B, Reiss AL, Menon V. Functional connectivity in the resting brain: a network analysis of the default mode hypothesis. *Proc Natl Acad Sci USA*. 2003; 100(1):253–258. [PubMed: 12506194]
39. Buckner RL, Snyder AZ, Shannon BJ, LaRossa G, Sachs R, Fotenos AF, Sheline YI, Klunk WE, Mathis CA, Morris JC, Mintun MA. Molecular, structural, and functional characterization of Alzheimer's disease: evidence for a relationship between default activity, amyloid, and memory. *J Neurosci*. 2005; 25(34):7709–7717. [PubMed: 16120771]
40. Habas C, Kamdar N, Nguyen D, Prater K, Beckmann CF, Menon V, Greicius MD. Distinct cerebellar contributions to intrinsic connectivity networks. *J Neurosci*. 2009; 29(26):8586–8594. [PubMed: 19571149]
41. Spiegel, H.; Spiegel, D. *Trance and Treatment: Clinical Uses of Hypnosis*. Washington, DC: American Psychiatric Publishing; 2004.
42. Glover GH, Lai S. Self-navigated spiral fMRI: interleaved versus single-shot. *Magn Reson Med*. 1998; 39(3):361–368. [PubMed: 9498591]
43. Poline JB, Worsley KJ, Evans AC, Friston KJ. Combining spatial extent and peak intensity to test for activations in functional imaging. *Neuroimage*. 1997; 5(2):83–96. [PubMed: 9345540]
44. Cohen, J. *Statistical Power Analysis for the Behavioral Sciences*. 2nd ed. Hillsdale, NJ: Erlbaum; 1988.
45. Talairach, J.; Tournoux, P. *Co-planar Stereotaxic Atlas of the Human Brain*. New York, NY: Thieme; 1988.
46. Whitfield-Gabrieli S, Thermenos HW, Milanovic S, Tsuang MT, Faraone SV, McCarley RW, Shenton ME, Green AI, Nieto-Castanon A, LaViolette P, Wojcik J, Gabrieli JD, Seidman LJ. Hyperactivity and hyperconnectivity of the default network in schizophrenia and in first-degree relatives of persons with schizophrenia. *Proc Natl Acad Sci USA*. 2009; 106(4):1279–1284. [PubMed: 19164577]
47. Good CD, Johnsrude IS, Ashburner J, Henson RN, Friston KJ, Frackowiak RS. A voxel-based morphometric study of ageing in 465 normal adult human brains. *Neuroimage*. 2001; 14(1, pt 1): 21–36. [PubMed: 11525331]
48. Basser PJ, Mattiello J, LeBihan D. MR diffusion tensor spectroscopy and imaging. *Biophys J*. 1994; 66(1):259–267. [PubMed: 8130344]
49. Woods RP, Grafton ST, Watson JD, Sicotte NL, Mazziotta JC. Automated image registration, II: intersubject validation of linear and nonlinear models. *J Comput Assist Tomogr*. 1998; 22(1):153–165. [PubMed: 9448780]
50. Jiang H, van Zijl PC, Kim J, Pearlson GD, Mori S. DtiStudio: resource program for diffusion tensor computation and fiber bundle tracking. *Comput Methods Programs Biomed*. 2006; 81(2): 106–116. [PubMed: 16413083]
51. Mori S, Kaufmann WE, Davatzikos C, Stieltjes B, Amodei L, Fredericksen K, Pearlson GD, Melhem ER, Solaiyappan M, Raymond GV, Moser HW, van Zijl PC. Imaging cortical association tracts in the human brain using diffusion-tensorbased axonal tracking. *Magn Reson Med*. 2002; 47(2):215–223. [PubMed: 11810663]
52. Mori S, Crain BJ, Chacko VP, van Zijl PC. Three-dimensional tracking of axonal projections in the brain by magnetic resonance imaging. *Ann Neurol*. 1999; 45(2):265–269. [PubMed: 9989633]
53. Williamson JW, McColl R, Mathews D, Mitchell JH, Raven PB, Morgan WP. Brain activation by central command during actual and imagined handgrip under hypnosis. *J Appl Physiol*. 2002; 92(3):1317–1324. [PubMed: 11842073]
54. Rainville P, Duncan GH, Price DD, Carrier B, Bushnell MC. Pain affect encoded in human anterior cingulate but not somatosensory cortex. *Science*. 1997; 277(5328):968–971. [PubMed: 9252330]
55. Vanhaudenhuyse A, Boly M, Baeteu E, Schnakers C, Moonen G, Luxen A, Lamy M, Degueldre C, Brichant JF, Maquet P, Laureys S, Faymonville ME. Pain and non-pain processing during hypnosis: a thulium-YAG event-related fMRI study. *Neuroimage*. 2009; 47(3):1047–1054. [PubMed: 19460446]
56. Posner MI, Petersen SE. The attention system of the human brain. *Annu Rev Neurosci*. 1990; 13:25–42. [PubMed: 2183676]

57. Frischholz EJ, Spiegel D, Trentalange MJ, Spiegel H. The Hypnotic Induction Profile and absorption. *Am J Clin Hypn.* 1987; 30(2):87–93. [PubMed: 3687817]
58. Kihlstrom JF, Register PA, Hoyt IP, Albright JS, Grigorian EM, Heindel WC, Morrison CR. Dispositional correlates of hypnosis: a phenomenological approach. *Int J Clin Exp Hypn.* 1989; 37(3):249–263. [PubMed: 2753575]
59. Bowers P. Hypnotizability, creativity and the role of effortless experiencing. *Int J Clin Exp Hypn.* 1978; 26(3):184–202. [PubMed: 689781]
60. Goldberg TE, Weinberger DR. Genes and the parsing of cognitive processes. *Trends Cogn Sci.* 2004; 8(7):325–335. [PubMed: 15242692]
61. Lichtenberg P, Bachner-Melman R, Gritsenko I, Ebstein RP. Exploratory association study between catechol-O-methyltransferase (COMT) high/low enzyme activity polymorphism and hypnotizability. *Am J Med Genet.* 2000; 96(6):771–774. [PubMed: 11121178]
62. Szekely A, Kovacs-Nagy R, Bányai EI, Gosi-Greguss AC, Varga K, Halmi Z, Ronai Z, Sasvari-Szekely M. Association between hypnotizability and the catechol-O-methyltransferase (COMT) polymorphism. *Int J Clin Exp Hypn.* 2010; 58(3):301–315. [PubMed: 20509070]
63. Spiegel, D. Intelligent design or designed intelligence? Hypnotizability as neurobiological adaptation. In: Nash, MR.; Barnier, AJ., editors. *The Oxford Handbook of Hypnosis: Theory, Research and Practice.* New York, NY: Oxford University Press; 2008. p. 179-199.
64. Spiegel H, Aronson M, Fleiss JL, Haber J. Psychometric analysis of the Hypnotic Induction Profile. *Int J Clin Exp Hypn.* 1976; 24(3):300–315. [PubMed: 1262087]
65. Stern DB, Spiegel H, Nee JC. The Hypnotic Induction Profile: normative observations, reliability and validity. *Am J Clin Hypn.* 1978; 21(2–3):109–133. [PubMed: 747161]
66. Spiegel D, Detrick D, Frischholz E. Hypnotizability and psychopathology. *Am J Psychiatry.* 1982; 139(4):431–437. [PubMed: 7065288]
67. Orne MT, Hilgard ER, Spiegel H, Spiegel D, Crawford HJ, Evans FJ, Orne EC, Frischholz EJ. The relation between the Hypnotic Induction Profile and the Stanford Hypnotic Susceptibility Scales, forms A and C. *Int J Clin Exp Hypn.* 1979; 27(2):85–102. [PubMed: 541133]
68. Frischholz EJ, Tryon WW, Fisher S, Maruffi BL, Vellios AT, Spiegel H. The relationship between the Hypnotic Induction Profile and the Stanford Hypnotic Susceptibility Scale, Form C: a replication. *Am J Clin Hypn.* 1980; 22(4):185–196. [PubMed: 7424797]
69. Frischholz EJ, Spiegel H, Tryon WW, Fisher S. The relationship between the Hypnotic Induction Profile and the Stanford Hypnotic Susceptibility Scale, Form C: revisited. *Am J Clin Hypn.* 1981; 24(2):98–105. [PubMed: 7340502]
70. DuHamel KN, Difede J, Foley F, Greenleaf M. Hypnotizability and trauma symptoms after burn injury. *Int J Clin Exp Hypn.* 2002; 50(1):33–50. [PubMed: 11778706]
71. Keuroghlian AS, Butler LD, Neri E, Spiegel D. Hypnotizability, posttraumatic stress, and depressive symptoms in metastatic breast cancer. *Int J Clin Exp Hypn.* 2010; 58(1):39–52. [PubMed: 20183737]
72. Spiegel D, Hunt T, Dondershine HE. Dissociation and hypnotizability in posttraumatic stress disorder. *Am J Psychiatry.* 1988; 145(3):301–305. [PubMed: 3344845]
73. Barry JJ, Atzman O, Morrell MJ. Discriminating between epileptic and nonepileptic events: the utility of hypnotic seizure induction. *Epilepsia.* 2000; 41(1):81–84. [PubMed: 10643928]
74. Pettinati HM, Kogan LG, Evans FJ, Wade JH, Home RL, Staats JM. Hypnotizability of psychiatric inpatients according to two different scales. *Am J Psychiatry.* 1990; 147(1):69–75. [PubMed: 2293791]
75. Frischholz EJ, Lipman LS, Braun BG, Sachs RG. Psychopathology, hypnotizability, and dissociation. *Am J Psychiatry.* 1992; 149(11):1521–1525. [PubMed: 1415819]
76. Spiegel D, Frischholz EJ, Fleiss JL, Spiegel H. Predictors of smoking abstinence following a single-session restructuring intervention with self-hypnosis. *Am J Psychiatry.* 1993; 150(7):1090–1097. [PubMed: 8317582]
77. Spiegel D, Frischholz EJ, Maruffi B, Spiegel H. Hypnotic responsivity and the treatment of flying phobia. *Am J Clin Hypn.* 1981; 23(4):239–247. [PubMed: 7282575]

78. Kosslyn SM, Cacioppo JT, Davidson RJ, Hugdahl K, Lovallo WR, Spiegel D, Rose R. Bridging psychology and biology: the analysis of individuals in groups. *Am Psychol*. 2002; 57(5):341–351. [PubMed: 12025764]
79. Ersche KD, Turton AJ, Pradhan S, Bullmore ET, Robbins TW. Drug addiction endophenotypes: impulsive versus sensation-seeking personality traits. *Biol Psychiatry*. 2010; 68(8):770–773. [PubMed: 20678754]
80. Canli T, Sivers H, Whitfield SL, Gotlib IH, Gabrieli JD. Amygdala response to happy faces as a function of extraversion. *Science*. 2002; 296(5576):2191. [PubMed: 12077407]
81. Davidson RJ. Empirical explorations of mindfulness: conceptual and methodological conundrums. *Emotion*. 2010; 10(1):8–11. [PubMed: 20141297]
82. Davidson RJ, Kabat-Zinn J, Schumacher J, Rosenkranz M, Muller D, Santorelli SF, Urbanowski F, Harrington A, Bonus K, Sheridan JF. Alterations in brain and immune function produced by mindfulness meditation. *Psychosom Med*. 2003; 65(4):564–570. [PubMed: 12883106]

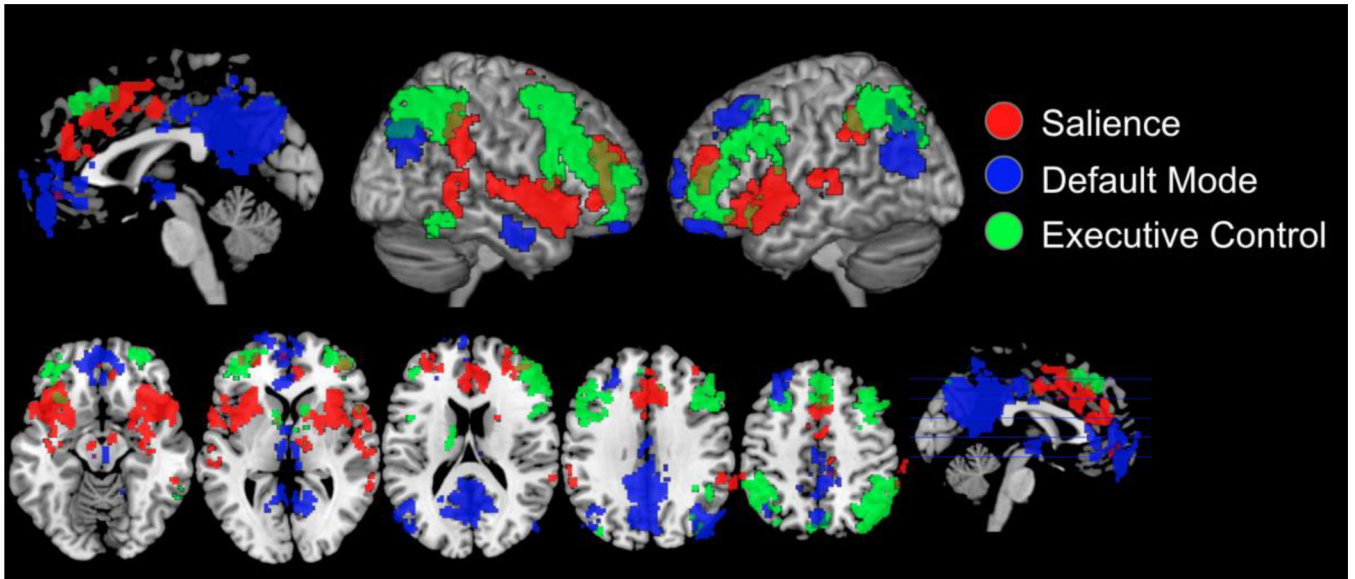


Figure 1. Templates used to select decomposed spatial maps for each network per subject

Author Manuscript

Author Manuscript

Author Manuscript

Author Manuscript

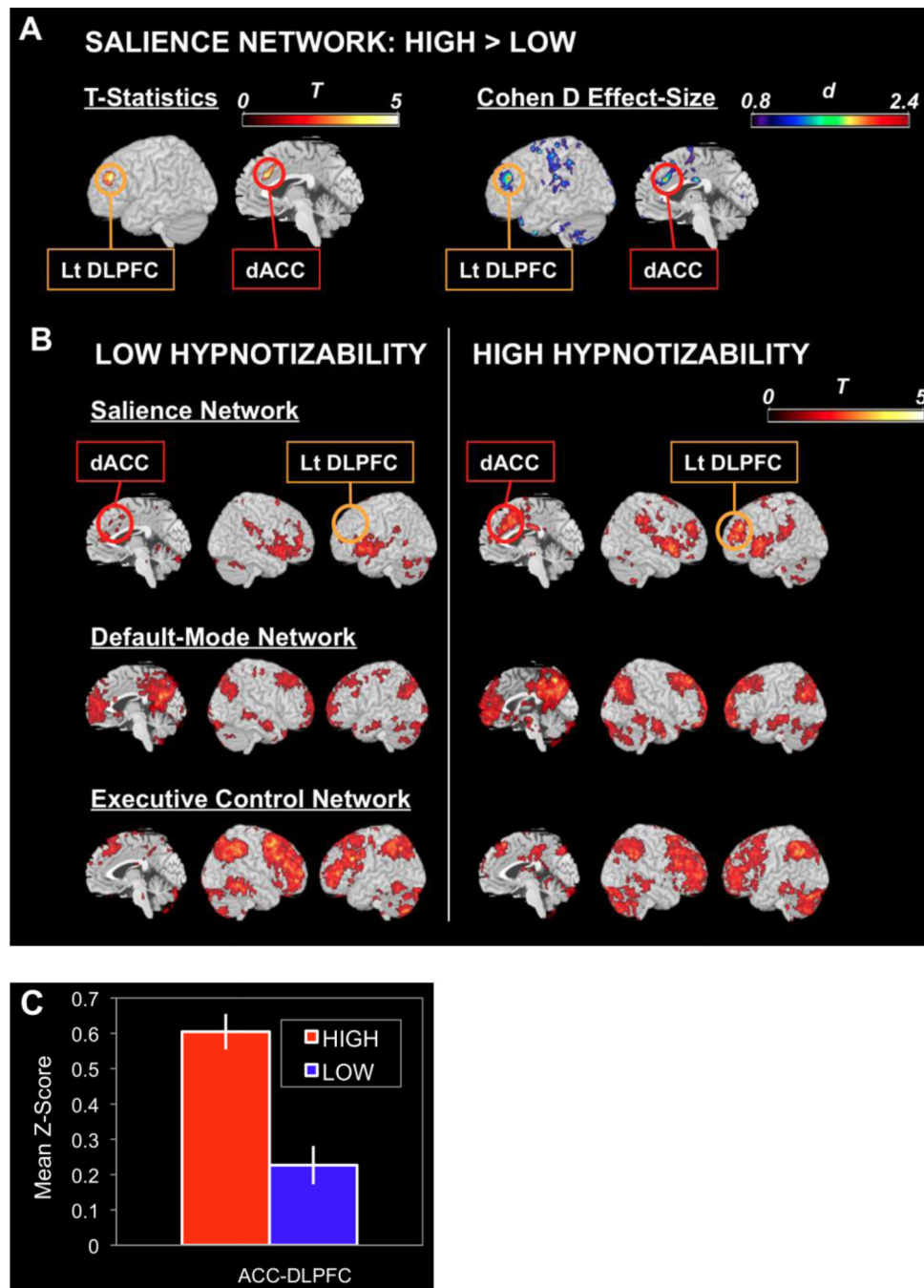


Figure 2. Functional connectivity in the HIGH and LOW groups

(A) Difference in ICA maps of the salience network between the HIGH and LOW groups. Brain regions that show significantly greater connectivity in HIGH compared to LOW using t-tests (left) and large effect-size (right).

(B) Significant clusters derived from one-sample t-tests of ICA maps for the salience, default-mode and executive-control networks for subjects with high and low hypnotizability (HIGH and LOW). Sagittal slices: $x=-2$ in Talairach coordinates. dACC: anterior cingulate cortex, DLPFC: dorsolateral prefrontal cortex.

(C) Seed-based correlations showing significant difference in functional dACC-DLPFC connectivity between the HIGH and LOW groups.

Author Manuscript

Author Manuscript

Author Manuscript

Author Manuscript

Table 1

Demographic information

	High		Low	
	Mean	SD	Mean	SD
Age	22.8	4.7	26.1	5.1
HIP	8.48	0.84	0.79	1.01
Gender (female:male)	6:6		6:6	
Handedness (left:right)	1:11		1:11	

HIP: Hypnotic Induction Profile

Author Manuscript

Author Manuscript

Author Manuscript

Author Manuscript

Significant clusters obtained from two-Sample *t*-tests showing significantly greater functional connectivity in the HIGH compared to the LOW group (see also Figure 2A).

Table 2

Brain Region	Brodmann Area	Talairach Coordinates			Z score	P value	Cluster Size (voxels)
		x	y	z			
Left Middle Frontal Gyrus (dorsolateral prefrontal cortex, DLPFC)	46,9,10	-40	40	22	4.036	0.01	191
Anterior Cingulate Cortex (ACC)	32,9	-2	29	26	3.891	0.004	247